

Confined variational calculation of *o*-Ps–He scattering properties

M.-S. Wu¹, J.-Y. Zhang^{1,2,3,*}, X. Gao², Y. Qian⁴, H.-H. Xie⁵, K. Varga⁶, Z.-C. Yan^{1,7} and U. Schwingenschlög³

¹State Key Laboratory of Magnetic Resonance and Atomic and Molecular Physics, Wuhan Institute of Physics and Mathematics, Chinese Academy of Sciences, Wuhan 430071, China

²Beijing Computational Science Research Center, Beijing 100193, China

³Physical Science and Engineering Division, King Abdullah University of Science and Technology, Thuwal 23955-6900, Saudi Arabia

⁴Department of Computer Science and Technology, East China Normal University, Shanghai 200062, China

⁵LSEC, ICMSEC, Academy of Mathematics and Systems Science, Chinese Academy of Sciences, Beijing 100190, China

⁶Department of Physics and Astronomy, Vanderbilt University, Nashville, Tennessee 37235, USA

⁷Department of Physics, University of New Brunswick, Fredericton, New Brunswick, Canada E3B 5A3



(Received 1 November 2019; accepted 25 March 2020; published 21 April 2020)

High-precision quantum-mechanical calculations have been developed to investigate positronium (Ps) scattering. Positronium scattering experiments are a powerful tool to study positronium-matter interactions, but the theoretical description of these experiments needs better accuracy. We have developed an *ab initio* confined variational approach that can reach higher collision energy, includes higher orbital momenta and uses small confining radii. Calculation of the Ps–He momentum-transfer cross section shows that the experimental Doppler broadening spectroscopy results are questionable. The energy dependence of the pickoff annihilation rate is also calculated, demonstrating an important role of the so far neglected *P*-wave contribution.

DOI: [10.1103/PhysRevA.101.042705](https://doi.org/10.1103/PhysRevA.101.042705)

I. INTRODUCTION

Positronium (Ps), a bound system of one electron and one positron, can be in a spin singlet state (*p*-Ps) with a lifetime of 0.125 ns and a spin triplet state (*o*-Ps) with a lifetime of 142 ns. It plays an important role for testing the theory of quantum electrodynamics [1–3], for generating antihydrogen [4,5], for realizing γ -ray lasers based on a Bose-Einstein condensate [6–9], for probing material defects [10–12], and for discovering phenomena beyond the standard model (such as dark matter) [13]. Experimental techniques exploring the Ps-matter interaction have significantly developed since the invention of the buffer gas positron trap [14]. Recent Ps beam experiments with He, Ar, Kr, Xe, H₂, N₂, O₂, and SF₆ have revealed electron-like scattering of Ps at intermediate energies [15] and unexpectedly small scattering cross sections have been observed for Ps-Ar and Ps-Xe scattering at low energies [16]. A theoretical understanding of these experiments is highly desirable, but accurate calculation of many-body Ps-atom scattering is very complicated.

Experimental measurements of the cross sections and annihilation rates have been carried out for Ps for many atoms and molecules [15–18]. Among them there are significant puzzles in the case of *o*-Ps–He scattering. For low energy *o*-Ps–He scattering, the momentum-transfer cross section (σ_m) has been determined experimentally by several approaches, including the Ps lifetime in liquid He (LMLHE) [19,20], the angular correlation of the annihilation radiation (ACAR) [21,22], and Doppler broadening spectroscopy (DBS) [23,24]. The lower limit of the ACAR results turns out to be close

to the LMLHE results but significantly higher than the DBS results. In addition, the energy dependence of σ_m is found to be linear by Coleman *et al.* [21] and quadratic by Engbrecht *et al.* [24]. Calculations [25–28] support the ACAR results while raising doubts about the DBS results. Experimental and theoretical efforts are required to reconcile these findings for collision energies between 0.3 and 1.2 eV.

Another important quantity for low-energy *o*-Ps–He scattering that is experimentally accessible is the pickoff annihilation rate (${}^1Z_{\text{eff}}$) [19,29–33], which represents the probability that the positron in Ps annihilates with an electron in He (the positron-electron pair should be in a spin singlet state) during the scattering process. Theoretical results are only available in the case of *S*-wave scattering at zero energy (${}^1Z_{0,\text{eff}}^0$) by Zhang *et al.* [25] and Green *et al.* [26]. The energy (or temperature) dependence of ${}^1Z_{\text{eff}}$ is crucial for interpreting precision Ps decay rate spectra taken in low and medium gas densities with thermodynamics processes [18,33]. The theoretical description of the energy dependence of ${}^1Z_{\text{eff}}$ is rather incomplete, as only *S*-wave scattering has been considered near-zero energy, despite continuous experimental efforts [19,32,33].

Theoretical determination of these quantities is very challenging due to the composite nature of both the target and projectile, the electron exchange between Ps and He, and the electron-electron and electron-positron correlations. The confined variational method (CVM), first developed by Mitroy *et al.* [34] and further developed by Zhang *et al.* [35], is an *ab initio* method to tackle low-energy elastic-scattering problems. CVM says that, if two potentials under the influence of the same confining potential have the same eigenenergy, then their phase shifts will be the same. Moreover, CVM tells us how to find a simple auxiliary potential which has the same phase shift as the equivalent potential between two atoms or

*jzhang@wipm.ac.cn

molecules. Two aspects of the method require improvement to address the topics of *o*-Ps–He scattering mentioned above: Elimination of unphysical effects of the confining potential (that acts on the center of mass of the positron and electron in He) and extension beyond *S*-wave scattering and to higher collision energies. Both these problems require significant extension of the quantum-mechanical calculations to the accurate description of scattering of complicated composite systems. These advancements are not restricted to Ps–He scattering, but other composite scattering experiments, including cold atom scattering and Ps-atom scattering, can also benefit from these efforts by using suitable pseudopotentials to manage the necessary degrees of freedom.

In this work, we first develop a strategy to effectively eliminate unphysical confining effects while extending the CVM to nonzero partial-wave scattering and higher collision energies. The advanced CVM is verified by calculating the *P*- and *D*-wave phase shifts for Ps–H scattering and comparing them with results of the complex Kohn variational method (CKVM) [36]. We then calculate the properties of *o*-Ps–He scattering: *S*-, *P*-, and *D*-wave phase shifts, momentum-transfer cross section, and energy dependence of the pickoff annihilation rate for *S* wave and *P* wave. We develop a computational method that allows us to use smaller confining regions and significantly improve the accuracy of the calculated scattering properties.

II. THEORY

Atomic units are used in the following unless stated otherwise. We consider the Schrödinger equations

$$\left(-\frac{\nabla^2}{2} + V_1(r)\right)\Psi(r) = E\Psi(r), \quad (1)$$

$$\left(-\frac{\nabla^2}{2} + V_1(r) + V_{\text{cp}}(r)\right)\Psi'(r) = E\Psi'(r), \quad (2)$$

$$\left(-\frac{\nabla^2}{2} + V_2(r)\right)\Phi(r) = E\Phi(r), \quad (3)$$

$$\left(-\frac{\nabla^2}{2} + V_2(r) + V_{\text{cp}}(r)\right)\Phi'(r) = E\Phi'(r), \quad (4)$$

where $E > 0$. V_1 represents the equivalent potential between Ps and He and V_2 represents the auxiliary potential. We assume

$$\begin{aligned} V_1(r) &= 0, & r > R_0, \\ V_2(r) &= 0, & r > R_0. \end{aligned} \quad (5)$$

The confining potential V_{cp} has the form

$$\begin{aligned} V_{\text{cp}}(r) &= 0, & r < R_0, \\ V_{\text{cp}}(r) &= G(r - R_0)^2, & r \geq R_0, \end{aligned} \quad (6)$$

where G is a tunable positive number. To achieve continuity of the four wave functions Ψ , Ψ' , Φ , and Φ' , their logarithmic derivatives

$$\Gamma_X(R_0) \equiv \left. \frac{1}{X(R_0)} \frac{dX}{dr} \right|_{R_0} \quad (7)$$

must be the same at energy E and radius R_0 [34], i.e.,

$$\Gamma_\Psi(R_0) = \Gamma_{\Psi'}(R_0) = \Gamma_\Phi(R_0) = \Gamma_{\Phi'}(R_0). \quad (8)$$

This implies that the phase shift as a function of $\Gamma_X(R_0)$ is exactly the same for Eqs. (1) and (3) at E . Although V_1 is not known, we can obtain the exact phase shift from Eq. (3).

In the approximation of infinite nucleus mass, the Schrödinger equation for *o*-Ps–He scattering has the form

$$\begin{aligned} H\Psi(\mathbf{r}, \mathbf{s}) &= E\Psi(\mathbf{r}, \mathbf{s}), \\ H &= -\sum_{i=1}^4 \frac{\nabla_i^2}{2} + \sum_{i=1}^4 \frac{Qq_i}{|\mathbf{r}_i|} \\ &\quad + \sum_i, j=1, j>i \frac{q_i q_j}{|\mathbf{r}_j - \mathbf{r}_i|}, \end{aligned} \quad (9)$$

where in $\mathbf{r}^T = (\mathbf{r}_1, \mathbf{r}_2, \mathbf{r}_3, \mathbf{r}_4)$ the positions of the electrons relative to the fixed nucleus are given by $\mathbf{r}_1, \mathbf{r}_2$, and \mathbf{r}_3 and the position of the positron is given by \mathbf{r}_4 . Similarly, $\mathbf{s}^T = (\mathbf{s}_1, \mathbf{s}_2, \mathbf{s}_3, \mathbf{s}_4)$ refers to the spin. Additionally, q_i is the charge of the i th lepton and Q is the charge of the nucleus. The total many-body wave function is expanded in the basis functions

$$\phi_n(\mathbf{r}, \mathbf{s}) = |\mathbf{v}|^{2K+L} \exp\left(-\frac{1}{2}\mathbf{r}^T A_n \mathbf{r}\right) Y_{LM}(\mathbf{v}) \chi(\mathbf{s}), \quad (10)$$

where $\mathbf{v} = u^T \mathbf{r}$, with $u^T = (u_1, u_2, u_3, u_4)$ being the global vector, and $\chi(\mathbf{s})$ is the spin function. K is an integer and can be chosen in our calculation. A_n is the n th parameter matrix. L is the total orbital angular momentum and Y_{LM} is the spherical harmonic. As compared with a spherical explicitly correlated Gaussian basis, the factor $|\mathbf{v}|^{2K+L}$ plays a key role in describing the increasing number of nodes of the wave function for Ps incident momentum $k > 0.2a_0^{-1}$. The global vector representation of the orbital angular momentum simplifies the calculation of matrix elements, because one-by-one coupling of the orbital angular momenta of the four leptons is avoided.

To eliminate unphysical confining effects, we consider the confining potentials

$$\sum_{i=1}^3 \mathcal{O}_T(i, 4) V_{\text{cp}}(\rho_i), \quad (11)$$

where $\rho_i = (|\mathbf{r}_i + \mathbf{r}_4|)/2$ and $\mathcal{O}_T(i, 4)$ is a spin-projection operator that ensures that only electron-positron pairs (electron i) in a spin triplet state are confined. According to Eq. (6), in the standard CVM the confining potentials act on both *o*-Ps and *p*-Ps. In our calculations, V_{cp} are replaced by Eq. (11). We define judgment indices

$$s_i^{nm} = \frac{\langle \phi_n | \mathcal{O}_T(i, 4) \Theta(r_{i4} - R_1) (r_{i4} - R_1)^2 | \phi_m \rangle}{\langle \phi_n | \mathcal{O}_T(i, 4) \Theta(\rho_i - R_0) (\rho_i - R_0)^2 | \phi_m \rangle}, \quad (12)$$

where $r_{i4} = |\mathbf{r}_i - \mathbf{r}_4|$, $\Theta(r_{i4} - R_1)$ is the Heaviside step function, and R_1 is a tunable number. If the confining potential acts on the pseudo Ps (formed by the positron and electron i in He), r_{i4} will be much larger than the characteristic size of Ps ($2a_0$). This means that s_i^{nm} will be a large value when R_1 is set to $2a_0$ (or a little larger). We discard $\langle \phi_n | \mathcal{O}_T(i, 4) V_{\text{cp}}(\rho_i) | \phi_m \rangle$ when s_i^{nm} exceeds a specific threshold. The effect of these two improvements [Eqs. (11) and (12)] is that we can perform the

TABLE I. Phase shifts (δ_k^L , in radians) calculated with present CVM and CKVM for Ps-H scattering. k is given in units of a_0^{-1} and a^b abbreviates $a \times 10^b$.

	CVM ($R_0 = 15a_0$)	CKVM [36]
$\delta_{0,1}^{3P}$	-1.72^{-3}	-1.72^{-3}
$\delta_{0,4}^{1D}$	5.15^{-2}	5.04^{-2}

calculation with smaller R_0 , which is opposite to the strategy of the standard CVM. In Ref. [35] unphysical confining effects have been removed by a large R_0 ($24a_0$ for Ps-H). The use of a small R_0 is the key point of our proposed method, providing two major advantages: First, we achieve better accuracy with fewer basis functions, since $\exp(-\frac{1}{2}\mathbf{r}^T\mathbf{A}\mathbf{r})$ decays quickly for growing r . In other words, for smaller R_0 in Eq. (5) it is easier to perform the calculation. Second, the CVM can reach higher collision energies due to the enhanced confinement.

III. RESULTS AND DISCUSSION

A. P - and D -wave phase shifts for Ps-H scattering

For Ps scattering from atoms and molecules, the CVM until now has been used only for calculating the S -wave phase shifts for Ps-H and Ps-H₂ scattering. To examine the reliability and efficiency of the present advanced CVM we study as an example the P - and D -wave phase shifts for Ps-H scattering; see Table I. Choosing $R_0 = 15a_0$ reduces the computation costs greatly as compared with previous calculations with $R_0 = 24a_0$. Because of the enhanced confinement, we can extract $\delta_{0,4}^{1D}$ ($1D$ -wave phase shift for $k = 0.4a_0^{-1}$) from the third bound state instead of higher bound states. Our CVM result of $\delta_{0,1}^{3P}$ ($3P$ -wave phase shift for $k = 0.1a_0^{-1}$) coincides with the CKVM result [36]. In the CKVM calculations, the value of $\delta_{0,4}^{1D}$ is less accurate than that of $\delta_{0,1}^{3P}$ because the mixed-symmetry basis functions are neglected for the D wave. For $\delta_{0,4}^{1D}$ our value is 2% higher than the CKVM value.

B. Phase shifts and momentum-transfer cross sections for o -Ps-He scattering

Phase shifts obtained by the present advanced CVM with $R_0 = 15a_0$ (sufficient because the distortion of Ps is predominant), many-body theory (MBT) [26], frozen-target model (FTM) [27], and free-electron-gas (FEG) approximation [28] are compared in Table II. In the energy range considered, the D -wave phase shifts obtained are much smaller than the S - and P -wave phase shifts (contribute little to σ_m) and are not shown here. The notations $\text{FTM}_{2.5}^{\text{vdW}}$, $\text{FTM}_{3.0}^{\text{vdW}}$, and $\text{FEG}_{2.5}^{\text{vdW}}$ mean that those calculations used a model van der Waals potential with a short-range cutoff function (the cutoff radius is $2.5a_0$, $3.0a_0$, and $2.5a_0$, respectively). There are obvious differences between our results and those of others, especially for the P wave, and the variations decrease with increasing k , which is due to the approximations entering the MBT, FTM, and FEG. The main advantage of our method compared with the MBT, FTM, and FEG is that we treat the electrons of Ps and He equally. This equivalence can be illustrated by the probability

TABLE II. Phase shifts (δ_k^L , in radians) calculated with present CVM, MBT [26], FTM [27], and FEG [28] for o -Ps-He scattering. k is given in units of a_0^{-1} and a^b abbreviates $a \times 10^b$.

	CVM ($R_0 = 15a_0$)	MBT	$\text{FTM}_{2.5}^{\text{vdW}}$	$\text{FTM}_{3.0}^{\text{vdW}}$	$\text{FEG}_{2.5}^{\text{vdW}}$
$\delta_{0,1}^S$	-1.57^{-1}	-1.69^{-1}	-1.52^{-1}	-1.61^{-1}	-1.61^{-1}
$\delta_{0,1}^P$	-9.88^{-4}	-1.84^{-3}	-6.62^{-4}	-1.25^{-3}	-3.72^{-3}
$\delta_{0,2}^S$	-3.15^{-1}	-3.34^{-1}	-3.02^{-1}	-3.20^{-1}	-3.24^{-1}
$\delta_{0,2}^P$	-7.16^{-3}	-1.33^{-2}	-5.29^{-3}	-9.47^{-3}	-1.18^{-2}
$\delta_{0,32}^S$	-5.03^{-1}	-5.22^{-1}	-4.77^{-1}	-5.07^{-1}	-5.21^{-1}
$\delta_{0,32}^P$	-3.09^{-2}	-4.51^{-2}	-2.13^{-2}	-3.48^{-2}	-4.54^{-2}
$\delta_{0,42}^S$	-6.52^{-1}	-6.67^{-1}	-6.16^{-1}	-6.57^{-1}	-6.85^{-1}
$\delta_{0,42}^P$	-6.55^{-2}	-8.32^{-2}	-4.62^{-2}	-6.94^{-2}	-9.64^{-2}

density distributions $C_i(R) = \int d\hat{\mathbf{R}} \langle \Psi(\mathbf{r}) | \delta(\mathbf{r}_i - \mathbf{R}) | \Psi(\mathbf{r}) \rangle$ of the electron and positron wave functions. Figure 1 shows results for S -wave scattering with $k = 0.1a_0^{-1}$. Interestingly, we observe $C_4/C_1 \approx 3$ for $R > 5a_0$, which can have two reasons: First, identity of the electrons implies $C_1 = C_2 = C_3$. Second, for large R the electrical neutrality of Ps requires that the sum of the probability density distributions of the electrons equals the probability density distribution of the positron, $C_1 + C_2 + C_3 = C_4$.

A comparison of theoretical and experimental results of σ_m is shown in Fig. 2. For $k < 0.2a_0^{-1}$ almost all theoretical values fall into the error bars of the experimental value of Nagashima *et al.* [22], with the best agreement provided by the $\text{FEG}_{2.5}^{\text{vdW}}$. The experimental values of Canter *et al.* [19], Rytola *et al.* [20], and Coleman *et al.* [21] are best approximated by the $\text{FTM}_{2.5}^{\text{vdW}}$ curve. Our CVM values fit better to the value of Coleman *et al.* [21] than to that of Nagashima *et al.* [22]. For $0.2a_0^{-1} < k < 0.42a_0^{-1}$, all theoretical values and the experimental values of Coleman *et al.* [21] are significantly higher than the experimental values of Skalsey *et al.* [23] and

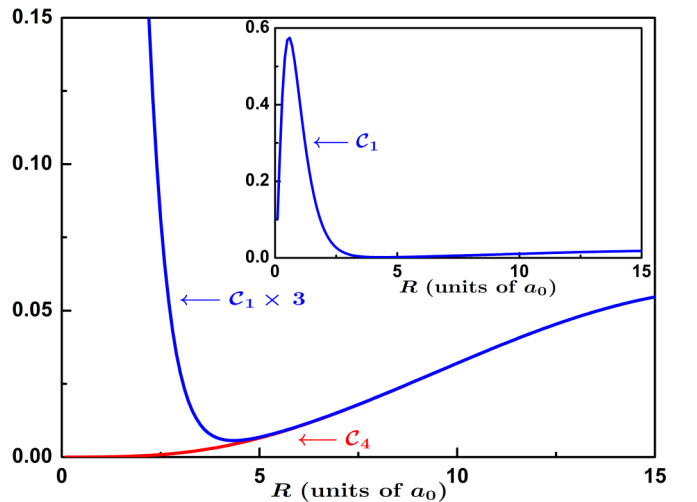


FIG. 1. Probability density distributions of the electron (C_1) and positron (C_4) wave functions for S -wave o -Ps-He scattering with $k = 0.1a_0^{-1}$. For $R > 5a_0$ we have $C_4/C_1 \approx 3$, i.e., the distortion of Ps can be neglected.

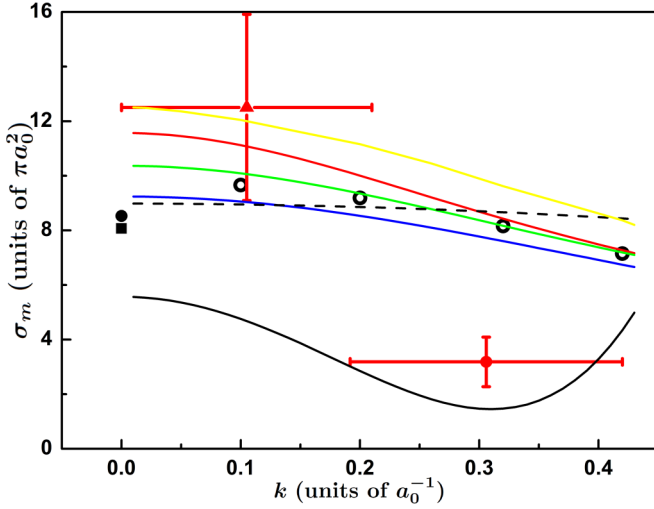


FIG. 2. Comparison of theoretical and experimental results of σ_m for *o*-Ps–He scattering. Theory: CVM with $R_0 = 15a_0$, open black circles; MBT, solid red line [26]; $\text{FTM}_{2,5}^{\text{vdW}}$, solid blue line [27]; $\text{FTM}_{3,0}^{\text{vdW}}$, solid green line [27]; $\text{FEG}_{2,5}^{\text{vdW}}$, solid yellow line [28]. Experiment: Canter *et al.*, filled black square [19]; Rytola *et al.*, filled black circle [20]; Coleman *et al.*, dash black line [21]; Nagashima *et al.*, filled red triangle [22]; Skalsey *et al.*, filled red circle [23]; Engbrecht *et al.*, solid black line [24].

Engbrecht *et al.* [24]. The only approximation in our work is that of infinite nucleus mass. We obtain $\delta_{0,1}^S = -0.15698$ in this case (values rounded in Table II) and $\delta_{0,1}^S = -0.15705$ for a nucleus mass of $m_{\text{He}} = 7294.299\,536\,1$ a.u. [37]. It can be estimated that the relative errors of δ_k^L and σ_m^k between infinite and finite nucleus mass are of the order of magnitude of $1/m_{\text{He}}$. Our *ab initio* calculation of σ_m therefore shows that the DBS results are questionable.

C. Pickoff annihilation rate for *o*-Ps–He scattering

After sufficient cooling, the dominant species left in the buffer gas is *o*-Ps. In addition to its own intrinsic decay (3γ process), *o*-Ps can decay through collision when the positron annihilates with the atomic (or molecular) electrons. The pickoff annihilation rate for *o*-Ps–He scattering represents the effective number of He electrons in a spin singlet state with the positron [17]. It is given by

$${}^1Z_{\text{eff}} = \langle \Psi | \sum_{i=1}^3 \mathcal{O}_S(i, 4) \delta(\mathbf{r}_i - \mathbf{r}_4) | \Psi \rangle, \quad (13)$$

where $\mathcal{O}_S(i, 4)$ is a spin projection operator that ensures that only electron-positron pairs (electron i) in a spin-singlet state annihilate. Accurate determination of ${}^1Z_{\text{eff}}$ requires a complete account of the short-range correlations and exchange effects. Partial-wave expansion gives

$${}^1Z_{\text{eff}} = \sum_L {}^1Z_{L,\text{eff}}, \quad (14)$$

and the effective-range theory [25] implies for *S*-wave scattering at small k that

$${}^1Z_{0,\text{eff}}(k) = {}^1Z_{0,\text{eff}}^0 + {}^1Z_{0,\text{eff}}^1 k^2 + {}^1Z_{0,\text{eff}}^2 k^4. \quad (15)$$

TABLE III. Comparison of theoretical and experimental results of ${}^1Z_{0,\text{eff}}^0$ for *o*-Ps–He scattering.

SVMSM [25]	MBT [26]	MBTEF [26]	FCSVM [38]
0.1157	0.0411	0.131	0.0378
Duff [29]	Smith [31]	Canter [19]	Coleman [30]
0.118 ± 0.016	0.116 ± 0.004	0.129 ± 0.006	0.125 ± 0.002
CVM($R_0 = 15a_0$)			
0.1197			

A comparison of theoretical and experimental results of ${}^1Z_{0,\text{eff}}^0$ is given in Table III. The results of MBT and FCSVM (fixed core stochastic variational method) underestimate ${}^1Z_{0,\text{eff}}^0$ by a factor of ≈ 3 . Including the enhancement factor (EF), which is an integral part of the MBT, the MBTEF value produces agreement with the experimental values of Duff *et al.* [29] and Canter *et al.* [19]. The stochastic variational method + stabilization method (SVMSM) gives values in agreement with the experimental values of Duff *et al.* [29] and Smith *et al.* [31]. By fitting the obtained values of ${}^1Z_{0,\text{eff}}^0$ using Eq. (15), we derive ${}^1Z_{0,\text{eff}}^0 = 0.1197$. This value is within the experimental error bars of Duff *et al.* [29] and Smith *et al.* [31].

To better understand the complex processes involved in the thermalization of Ps in gases, it is essential to determine the energy (or temperature) dependence of ${}^1Z_{\text{eff}}$. Vallery *et al.* [33] have found that ${}^1Z_{\text{eff}}$ increases linearly with the scattering energy, while no energy dependence was observed by Fox *et al.* [32]. Theoretically, only ${}^1Z_{0,\text{eff}}$ has been investigated near zero energy. To resolve this long-standing puzzle, we calculate ${}^1Z_{1,\text{eff}}$, neglecting the contribution of ${}^1Z_{2,\text{eff}}$, i.e., only *S*- and *P*-wave contributions are taken into account, ${}^1Z_{\text{eff}} = {}^1Z_{0,\text{eff}} + {}^1Z_{1,\text{eff}}$. To normalize the probability density distributions of Ps we use the asymptotic forms $\sin^2(kR + \delta_k^S)$ and $\sin^2(kR - \pi/2 + \delta_k^P)$ for the *S*- and *P*-wave contributions, respectively. Our results are shown in Fig. 3. For increasing k , ${}^1Z_{0,\text{eff}}$ decreases slowly but ${}^1Z_{1,\text{eff}}$ increases quickly, i.e., the *P*-wave contributions become more and more important. By

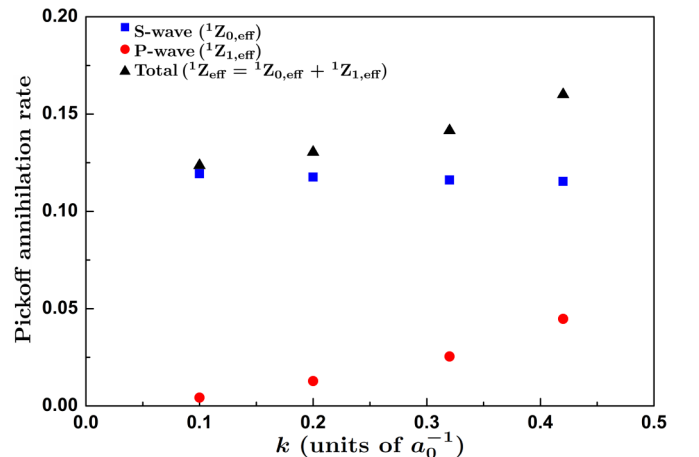


FIG. 3. Momentum dependence of the pickoff annihilation rate for *o*-Ps–He scattering.

the effect of ${}^1Z_{1,\text{eff}}$, ${}^1Z_{\text{eff}}$ increases with k . We find that ${}^1Z_{\text{eff}}$ is a factor of 1.3 larger at $k = 0.42a_0^{-1}$ than at $k = 0.1a_0^{-1}$, implying that the positron annihilates significantly easier. We suggest that this important effect must be taken into account in the determination of σ_m from the experiments of Skalsey *et al.* [23] and Engbrecht *et al.* [24], as it may be the key point to explain the unexpectedly small σ_m .

IV. SUMMARY

To resolve long-standing questions in the context of low-energy *o*-Ps–He scattering, we have improved the CVM by eliminating unphysical confining effects and extending it beyond *S*-wave scattering and to higher collision energies. The key point of our proposed method is the usage of a small R_0 , which is opposite to the strategy of the standard CVM. We present *ab initio* calculations of σ_m and ${}^1Z_{\text{eff}}$ for *o*-Ps–He scattering in the energy range from 0 to 1.2 eV. Our accurate values of σ_m clarify that its energy dependence is almost linear, rendering previous DBS results questionable. *P*-wave contributions to ${}^1Z_{\text{eff}}$ are considered for the first time, which makes it possible to obtain the energy dependence of ${}^1Z_{\text{eff}}$. Our results suggest that the energy dependence of ${}^1Z_{\text{eff}}$ influences the determination of σ_m from DBS experiments.

Besides positron and Ps scattering, there is an increasing demand for accurate determination of the low-energy scattering properties between atoms and molecules as the development of the ultracold atomic and molecular physics. For example, the He-He and He-Li scattering lengths are important for understanding the Efimov effect and the Li-H₂ scattering cross section is key for creating a cold-atom vacuum standard device. Our proposed method makes it possible to accurately study the low-energy scattering properties of these complicated systems.

ACKNOWLEDGMENTS

M.-S.W. was supported by the National Natural Science Foundation of China under Grant No. 11704399. J.-Y.Z. was supported by the “Hundred Talents Program” of the Chinese Academy of Sciences. Z.-C.Y. was supported by the NSERC of Canada and in part by the Chinese Academy of Sciences within the CAS/SAFEA International Partnership Program for Creative Research Teams. The research reported in this publication was supported by funding from King Abdullah University of Science and Technology (KAUST). The authors are thankful for the computational resources provided by the ACEnet of Canada.

-
- [1] S. G. Karshenboim, *Phys. Rep.* **422**, 1 (2005).
 - [2] T. Yamazaki, A. Miyazaki, T. Suehara, T. Namba, S. Asai, T. Kobayashi, H. Saito, I. Ogawa, T. Idehara, and S. Sabchevski, *Phys. Rev. Lett.* **108**, 253401 (2012).
 - [3] G. S. Adkins, M. Kim, C. Parsons, and R. N. Fell, *Phys. Rev. Lett.* **115**, 233401 (2015).
 - [4] G. Gabrielse, R. Kalra, W. S. Kolthammer, R. McConnell, P. Richerme, D. Grzonka, W. Oelert, T. Seifzick, M. Zielinski, D. W. Fitzakerley *et al.* (ATRAP Collaboration), *Phys. Rev. Lett.* **108**, 113002 (2012).
 - [5] A. S. Kadyrov, C. M. Rawlins, A. T. Stelbovics, I. Bray, and M. Charlton, *Phys. Rev. Lett.* **114**, 183201 (2015).
 - [6] D. B. Cassidy, V. E. Meline, and A. P. Mills, *Phys. Rev. Lett.* **104**, 173401 (2010).
 - [7] H. K. Avetissian, A. K. Avetissian, and G. F. Mkrtchian, *Phys. Rev. Lett.* **113**, 023904 (2014).
 - [8] D. B. Cassidy, *Eur. Phys. J. D* **72**, 53 (2018).
 - [9] A. P. Mills, *Phys. Rev. A* **100**, 063615 (2019).
 - [10] M. J. Puska and R. M. Nieminen, *Rev. Mod. Phys.* **66**, 841 (1994).
 - [11] F. Tuomisto and I. Makkonen, *Rev. Mod. Phys.* **85**, 1583 (2013).
 - [12] C. Hugenschmidt, *Surf. Sci. Rep.* **71**, 547 (2016).
 - [13] C. Frugiuele, J. Pérez-Ríos, and C. Peset, *Phys. Rev. D* **100**, 015010 (2019).
 - [14] C. M. Surko, M. Leventhal, and A. Passner, *Phys. Rev. Lett.* **62**, 901 (1989).
 - [15] S. J. Brawley, S. Armitage, J. Beale, D. E. Leslie, A. I. Williams, and G. Laricchia, *Science* **330**, 789 (2010).
 - [16] S. J. Brawley, S. E. Fayer, M. Shipman, and G. Laricchia, *Phys. Rev. Lett.* **115**, 223201 (2015).
 - [17] P. A. Fraser, *Adv. At. Mol. Phys.* **4**, 63 (1968).
 - [18] M. Skalsey, J. J. Engbrecht, R. K. Bithell, R. S. Vallery, and D. W. Gidley, *Phys. Rev. Lett.* **80**, 3727 (1998).
 - [19] K. F. Canter, J. D. McNutt, and L. O. Roellig, *Phys. Rev. A* **12**, 375 (1975).
 - [20] K. Rytola, J. Vettenranta, and P. Hautojarvi, *J. Phys. B: At. Mol. Phys.* **17**, 3359 (1984).
 - [21] P. G. Coleman, S. Rayner, F. M. Jacobsen, M. Charlton, and R. N. West, *J. Phys. B: At., Mol. Opt. Phys.* **27**, 981 (1994).
 - [22] Y. Nagashima, T. Hyodo, K. Fujiwara, and A. Ichimura, *J. Phys. B: At., Mol. Opt. Phys.* **31**, 329 (1998).
 - [23] M. Skalsey, J. J. Engbrecht, C. M. Nakamura, R. S. Vallery, and D. W. Gidley, *Phys. Rev. A* **67**, 022504 (2003).
 - [24] J. J. Engbrecht, M. J. Erickson, C. P. Johnson, A. J. Kolan, A. E. Legard, S. P. Lund, M. J. Nyflot, and J. D. Paulsen, *Phys. Rev. A* **77**, 012711 (2008).
 - [25] J. Y. Zhang and J. Mitroy, *Phys. Rev. A* **78**, 012703 (2008).
 - [26] D. G. Green, A. R. Swann, and G. F. Gribakin, *Phys. Rev. Lett.* **120**, 183402 (2018).
 - [27] A. R. Swann and G. F. Gribakin, *Phys. Rev. A* **97**, 012706 (2018).
 - [28] R. S. Wilde and I. I. Fabrikant, *Phys. Rev. A* **98**, 042703 (2018).
 - [29] B. G. Duff and F. F. Heyman, *Proc. Phys. Soc. London* **517**, 281 (1962).
 - [30] P. G. Coleman, T. C. Griffith, G. R. Heyland, and T. L. Killeen, *J. Phys. B: At. Mol. Phys.* **8**, L185 (1975).
 - [31] J. B. Smith, J. D. McGervey, and A. J. Dahm, *Phys. Rev. B* **15**, 1378 (1977).
 - [32] R. A. Fox, K. F. Canter, and M. Fishbein, *Phys. Rev. A* **15**, 1340 (1977).

- [33] R. S. Vallery, A. E. Leanhardt, M. Skalsey, and D. W. Gidley, *J. Phys. B: At., Mol. Opt. Phys.* **33**, 1047 (2000).
- [34] J. Mitroy, J. Y. Zhang, and K. Varga, *Phys. Rev. Lett.* **101**, 123201 (2008).
- [35] J.-Y. Zhang, Z.-C. Yan, and U. Schwingenschlögl, *Europhys. Lett.* **99**, 43001 (2012).
- [36] D. Woods, S. J. Ward, and P. Van Reeth, *Phys. Rev. A* **92**, 022713 (2015).
- [37] P. J. Mohr, B. N. Taylor, and D. B. Newell, *Rev. Mod. Phys.* **84**, 1527 (2012).
- [38] J. Mitroy and I. A. Ivanov, *Phys. Rev. A* **65**, 012509 (2001).